PHYSICAL REVIEW A, VOLUME 65, 030702(R)

Simultaneous charge polarization and fragmentation of N_2 molecules in slow keV collisions with Kr^{8+} ions

M. Ehrich, U. Werner, and H. O. Lutz
Fakultät für Physik, Universität Bielefeld, D-33501 Bielefeld, Germany

T. Kaneyasu, K. Ishii, and K. Okuno
Department of Physics, Tokyo Metropolitan University, 192-0397 Tokyo, Japan

U. Saalmann
Max-Planck-Institut für Physik komplexer Systeme, Nöthnitzer Strasse 38, D-01187 Dresden, Germany

(Received 30 August 2001; published 11 February 2002)

Coulomb fragmentation processes in collisions of Kr^{8+} ions with nitrogen molecules were studied at projectile energies between 19 and 171 eV/u. At low impact energies ($\lesssim 50$ eV/u) and small impact parameters, the electron distribution of the fragmenting molecular N_2^{q+} ion becomes strongly polarized. This is due to the presence of the slow highly charged projectile *during* the fragmentation process. Microscopic calculations simultaneously incorporating electron transfer and molecular dissociation give insight into the dynamics of this newly found polarization effect.

DOI: 10.1103/PhysRevA.65.030702 PACS number(s): 34.50.Gb, 34.70.+e

The study of Coulomb fragmentation processes in collisions of molecules with ions is not only of fundamental interest but also of great importance in wide areas of science and technology. Examples are astrophysics, biophysics, and molecular physics where such data help to shed light on problems as diverse as processes in interstellar gases, the upper layers of stars and gas giant atmospheres [1,2], the damage to biological tissue by energetic radiation [3], and the direct determination of molecular structures from Coulomb explosion experiments [4,5]. An extensive literature deals with such fragmentation phenomena, spanning a wide range of projectile and target species as well as collision energies (for a collection of recent papers, cf., e.g., [6–8], and references therein).

Such studies are generally based on a crucial assumption which greatly facilitates the interpretation of results: collisional ionization and fragmentation can be treated as two independent processes. In a recent paper by Ali *et al.* [9], evidence has been seen of a breakdown of this model. In collisions of D_2 with Xe^{26+}, the molecular fragment momentum distribution is distorted by the presence of the projectile ion. In this paper, we report on direct experimental evidence, supported by *ab initio* calculations, of a new many-body effect: in charge-changing collisions of slow highly charged Kr^{8+} ions with N_2, the molecular electron distribution is strongly polarized by the presence of the highly charged ion, and the molecule fragments while the projectile is still nearby.

The experiment concentrates on electron capture by very slow Kr^{8+} ions in collisions with N_2. Figure 1 shows a schematic view of the setup. Krypton ions of energies between 19 and 171 eV/u are produced in a Mini-EBIS (Electron Beam Ion Source) [10], mass-selected and collimated to a narrow beam of 1 mm in diameter. In the interaction chamber, they collide with a N_2 gas target which is emitted from a nozzle. Quite importantly, this chamber is field-free to avoid an undesired deflection of the slow, highly charged projectiles. Molecular fragment ions which are emitted back-to-back and perpendicular to the projectile direction leave the collision chamber and are post-accelerated by 150 V; they are collected by two OctoPole Ion-beam Guides (OPIG [11], acceptance solid angle of $4\pi/12$) which guide them to channeltron detectors. The post-acceleration improves the OPIG transmission, the identification of the fragment charge, and it eliminates a possible (weak) dependence of the detection efficiency on the fragmentation energy. The projectile ions are separated according to their charge state in an electrostatic analyzer and detected in a microchannel plate arrangement (chevron configuration). A thin (1 mm) horizontal slit in front of this analyzer limits projectile detection to such

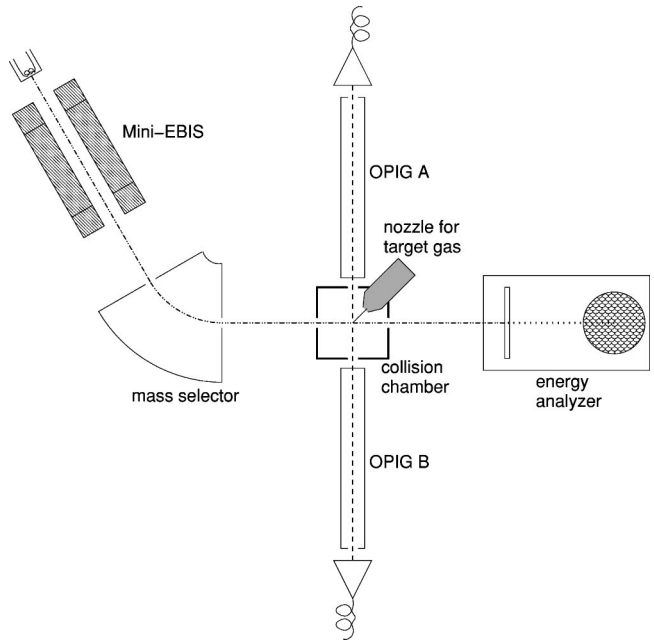

FIG. 1. Experimental setup (top view).

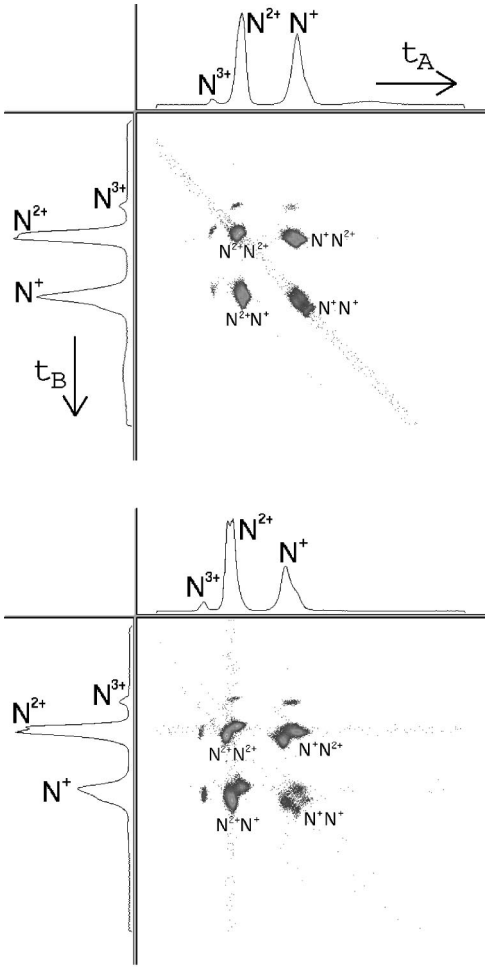

FIG. 2. Coincidence maps for 95.2 eV/u Kr^{8+} (upper) and 19.0 eV/u Kr^{8+} (lower) ion impact leading to Kr^{6+} and N^{p+},N^{q+} products. t_A,t_B refer to the time-of-flight of fragments detected in OPIG *A* and *B*, respectively.

events in which the collisionally transferred momentum lies close to the plane defined by the ion beam and the OPIG axes (scattering angle in the center-of-mass system $<4.5°$). The coincidence electronics is triggered by the projectile (start pulse), and the fragment ions generate the stop signals. Two correlated time-of-flight measurements are obtained for each molecular fragmentation.

To gain insight into the dynamics of an individual collision process, we have performed nonadiabatic quantum molecular dynamics (NA-QMD) calculations [12] which simultaneously and self-consistently treat the involved electronic and nuclear degrees of freedom. For the collisions studied here, this comprises classical molecular dynamics for all three atomic cores coupled to the quantum dynamics (in terms of Kohn-Sham equations) of the ten valence electrons of N_2, cf. also [13]. A recent numerical realization of this approach based on an approximate treatment of the electronic equations has proven to be useful in the interpretation of charge transfer collisions of metal clusters with neutral [13] as well as laser-polarized [14] atomic targets. The current implementation solves the highly nonlinear Kohn-Sham equations and thus allows for the description of collisions

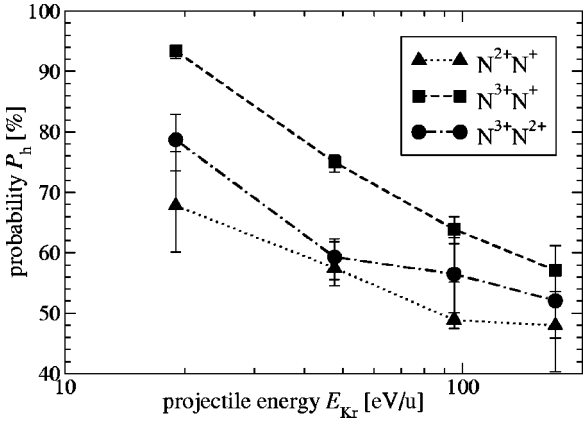

FIG. 3. Probability P_h of $N^{2+}N^+$, $N^{3+}N^+$, and $N^{3+}N^{2+}$ dissociations where the higher charged fragment is the faster one. The error bars indicate the fluctuations in several measurements. In the case of isotropic fragmentations, a probability of 50% is expected.

with highly charged ions and the induced multiple electron transfer processes. Details of the numerical procedure will be reported elsewhere [15].

In the present paper, we concentrate on the following reaction:

$$Kr^{8+} + N_2 \rightarrow Kr^{(8-i+r)+} + N^{p+} + N^{q+} + re^-$$

with $p+q=i>r$. As an example, Fig. 2 shows coincidence maps for 95.2 eV/u and 19.0 eV/u Kr^{8+} ion impact leading to Kr^{6+} charge-changed projectiles and N^{p+},N^{q+} products. Coincidences between fragment ion pairs with a total charge of up to 5+ (i.e., $N^{3+}N^{2+}$ pairs) can be distinguished. To explain the details of these correlation features, we note that in the target center-of-mass frame of a free N_2 molecular ion, both fragments N^{p+},N^{q+} move apart with the same velocity. Pairs of equally charged (''symmetric,'' $p=q$) fragments will (after post-acceleration) thus be detected after equal flight times if their center of mass is initially at rest. As a consequence, for such symmetric fragmentations the spread of the coincidence peaks *parallel* to the diagonal in Fig. 2 corresponds to the kinetic energy distribution of the fragmentation process; for asymmetrically charged fragment pairs, the situation is qualitatively similar although they will be displaced from the diagonal due to the different post-acceleration of the two fragments before they enter the OPIGs. Furthermore, the flight time difference of correlated pairs (i.e., the width of the coincidence peaks *perpendicular* to the diagonal in Fig. 2) contains information on the target center-of-mass motion [16] : instead of two fragments having equal dissociation velocities v_{diss} in the laboratory frame, a ''slow'' $(v_{\mathrm{diss}}-v)$ fragment will reach one OPIG and a ''fast'' $(v_{\mathrm{diss}}+v)$ fragment the other, with v the CMS velocity parallel to the OPIG axes; the coincident ''back-to-back'' detection of both fragments thus allows indentification of the fragment which in the collision has been nearer to the projectile (i.e., the ''slow'' fragment). We recall now that the experimental setup allows coincident detection of only such fragment ion pairs which have received a collisional recoil momentum into the direction of either one of the two OPIGs.

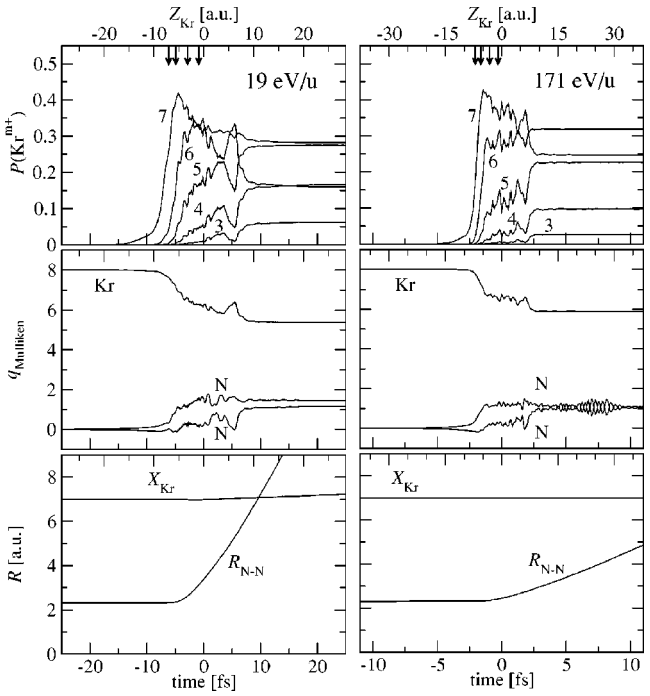

FIG. 4. Probabilities P for various projectile charge states Kr^{m+} (upper row), the atomic Mulliken charges [23] q (middle row), and the intramolecular distance $R_{N\text{-}N}$ as well as the projectile coordinate X_{Kr} in the scattering plane perpendicular to the beam (lower row) as a function of the time for collision events with coplanar collision geometry ($b=7$ a.u.) at 19 eV/u (left column) and 171 eV/u (right) impact energy, respectively, as obtained from NA-QMD calculations. On the top, the coordinate Z_{Kr} of the projectile along the beam axis is given. The arrows mark the critical distances as obtained from the overbarrier model [21,22].

This gives rise to a splitting of the coincidence ''blobs'' in Fig. 2 (particularly noticeable at the lower impact energy): each half of the ''blob'' is displaced from the center by the mean collisional momentum transfer in the direction of either OPIG *A* or *B*, respectively. Similar to the COLTRIMS-technique [17,18], this collision-induced motion of the target center of mass may be used to derive the related scattering angle and, thus, angle-dependent relative low-energy charge exchange cross sections for well-defined initial and final projectile charges as well as molecular ion charges. This will be the subject of a separate publication.

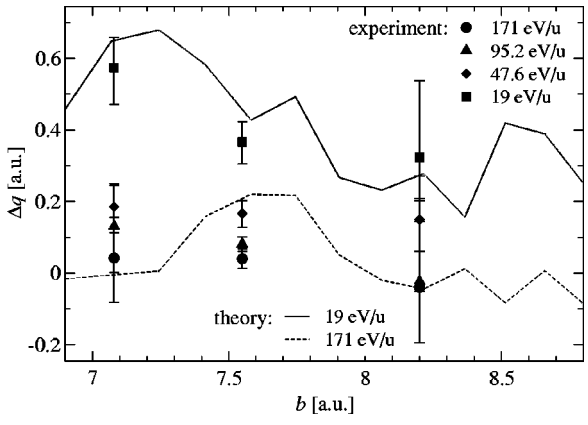

FIG. 5. Averaged charge difference $\overline{\Delta q}$ inside the molecular ion at different collision energies. The error bars indicate the fluctuations in several measurements. The lines show the charge differences as obtained from NA-QMD calculations for a coplanar collision geometry.

The most interesting aspect of these results, however, is the unequal strength of the two halves of the coincidence ''blobs'' in case of asymmetrically charged fragments ($p \neq q$), as seen, e.g., in Fig. 2 at the lowest collision energy (19 eV/u) [19]. Inspection of experimental data as shown in Fig. 2 reveals a tendency of the slower fragment (i.e., the fragment which has been nearer to the projectile) to carry the smaller positive charge. This is interpreted by the presence of the highly charged projectile *during* the fragmentation process. In Fig. 3, we show for asymmetric fragmentation processes the probability P_h for fragmentations in which the faster fragment is the more highly charged one, i.e., $P_h = n_h/(n_h+n_l)$ with n_h and n_l the number of faster fragments which carry the higher and lower charge, respectively.

To elucidate the collision dynamics in more detail, we have performed NA-QMD calculations. However, as prohibitive numerical calculations are required to account for all possible target orientations and impact parameters, we restrict the theoretical investigations to coplanar collision geometries with the molecule perpendicular to the beam axis at various impact parameters. As a typical example, Fig. 4 shows the time dependence of calculated collision events with an impact parameter of $b=7$ a.u. at the lowest and the highest energy measured. First of all, one notices that in the case of very slow projectiles (left column of Fig. 4), the collision time (i.e., the characteristic time of electronic transitions, here ~ 20 fs) becomes comparable to the fragmentation time (e.g., where the molecule doubles its bond length, here ~ 10 fs). As can be seen for 19 eV/u in the lower and upper left panel, electron transfer still occurs at times around $t \sim 5$ fs while the intramolecular distance $R_{N\text{-}N}$ is already about twice the N_2 bond length. This effect is generally neglected in the comparatively swift collisions reported in the literature and disappears at the higher energy of 171 eV/u. In this case, the projectile has already left the interaction region when the molecule has doubled its bond length (at $t \sim 10$ fs with $Z_{Kr} > 30$ a.u., cf. right column). The time evolution of the probabilities $P(Kr^{m+})$ of the projectile charge $m=7,\ldots,3$ in Fig. 4 reveals that the electron transfer from the molecule occurs stepwise as also assumed in the classical overbarrier model [20,21], and the critical distances (marked by arrows in the upper row) of the model by Niehaus [21,22] are even quantitatively confirmed. In addition, the calculations also show clearly the strong polarization of the N_2 molecule by the presence of the highly charged projectile (middle frames of Fig. 4). At the lower energy, this polarization becomes noticeable already during the projectile approach to the target ($t \lesssim -10$ fs), it is maximum during the interaction ($t \sim -10$ to $+10$ fs), and it finally leads to a nonvanishing value Δq when the molecule fragments and is still subjected to the Coulomb field of the projectile ($t \gtrsim +10$ fs).

In order to compare the calculations with the experiment, we use the charges q_f and q_s of the faster and the slower fragment ion, respectively, and determine the averaged charge difference

$$\overline{\Delta q} = \frac{1}{n} \sum_{i=1}^{n} [q_f(i) - q_s(i)],$$

with i running over all n measured fragmentations $N^{q_f+} + N^{q_s+}$ with $q_f(i) + q_s(i) = 3$, 4, and 5. These averaged charge differences are plotted at the largest impact parameters which one would expect from the overbarrier model [21,22] for the capture of three, four, or five electrons along with theoretical results from the coplanar collision geometry for 19 eV/u and 171 eV/u (Fig. 5). Processes with more than five captured electrons which are expected at smaller impact parameters were hardly observed. Both, the calculations and experimental results show that the charge difference of the two nitrogen ions increases with decreasing impact parameter. Comparing the data at various collision energies, we find that the charge difference increases with decreasing projectile velocity, which can be explained by the longer interaction time.

In summary, we studied the dissociation of nitrogen molecules in collisions with Kr^{8+} ions in the energy range of 19 eV/u to 171 eV/u. The time-of-flight of both fragment ions was measured in coincidence with the final projectile charge state. At collision energies below about 50 eV/u, the molecular ionization and fragmentation can no longer be separated into two independent steps. The presence of the highly charged projectile causes a polarization of the target electron distribution such that the fragment which is closer to the projectile tends to carry the lower charge. This effect increases with a higher ionization state of the target molecule. This has been explained by microscopic calculations. Further insight may be expected from a systematic experimental and theoretical study that is currently underway.

We are grateful to N.M. Kabachnik for valuable discussions and comments. This work was supported by the Deutsche Forschungsgemeinschaft, the Japan Society for the Promotion of Science, and by the EU Infrastructure Cooperation Network HRPI-1999-40012 (LEIF).

[1] W. Liu and D.R. Schultz, Astrophys. J. **526**, 538 (1999).
[2] J.F. Cooper *et al.*, Icarus **149**, 133 (2001).
[3] G.H. Olivera *et al.*, Phys. Med. Biol. **43**, 2347 (1998).
[4] Z. Vager and E.P. Kanter, Nucl. Instrum. Methods Phys. Res. B **33**, 98 (1988); Z. Vager, R. Naaman, and E.P. Kanter, Science **244**, 426 (1989); Z. Vager, T. Graber, E.P. Kanter, and D. Zaijfman, Phys. Rev. Lett. **70**, 3549 (1993).
[5] U. Werner, K. Beckord, J. Becker, and H.O. Lutz, Phys. Rev. Lett. **74**, 1962 (1995).
[6] C.J. Latimer, Adv. At., Mol., Opt. Phys. **30**, 105 (1993).
[7] H.O. Folkerts, F.W. Bliek, M.C. de Jong, R. Hoekstra, and R. Morgenstern, J. Phys. B **30**, 5833 (1997); H.O. Folkerts, T. Schlathölter, R. Hoekstra, and R. Morgenstern, *ibid.* **30**, 5849 (1997).
[8] B. Siegmann, U. Werner, R. Mann, N.M. Kabachnik, and H.O. Lutz, Phys. Rev. A **62**, 022718 (2000).
[9] I. Ali *et al.*, R.D. DuBois, C.L. Cocke, S. Hagmann, C.R. Feeler, and R.E. Olson, Phys. Rev. A **64**, 022712 (2001).
[10] K. Okuno, K. Soejima, and Y. Kaneko, Nucl. Instrum. Methods Phys. Res. B **53**, 387 (1991).
[11] K. Okuno, J. Phys. Soc. Jpn. **55**, 1504 (1986).
[12] U. Saalmann and R. Schmidt, Z. Phys. D: At., Mol. Clusters **38**, 153 (1996); Phys. Rev. Lett. **80**, 3213 (1998).
[13] O. Knospe, J. Jellinek, U. Saalmann, and R. Schmidt, Phys. Rev. A **61**, 022715 (2000).
[14] Z. Roller-Lutz, Y. Wang, H.O. Lutz, U. Saalmann, and R. Schmidt, Phys. Rev. A **59**, R2555 (1999).
[15] U. Saalmann (unpublished).
[16] The broadening caused by experimental effects, as, e.g., the width of the projectile beam, is significantly smaller than observed.
[17] A. Dörner *et al.*, Nucl. Instrum. Methods Phys. Res. B **124**, 225 (1997).
[18] M.A. Abdallah *et al.*, Phys. Rev. A **57**, 4373 (1998).
[19] Since both halves result from double coincidence measurements of the same fragmentation channel, the intensity difference is not a consequence of detection effiencies because the ion charges are the same and the velocities differs insignificantly due to the post-acceleration.
[20] A. Bárány *et al.*, Nucl. Instrum. Methods Phys. Res. B **9**, 397 (1985).
[21] A. Niehaus, J. Phys. B **19**, 2925 (1986).
[22] For the ionization potentials needed in the overbarrier model, we used the values from static NA-QMD calculations.
[23] We use the standard definition of charges in molecules due to Mulliken; see, e.g., A. Szabo and N. S. Ostlund, *Modern Quantum Chemistry* (McGraw-Hill, New York, 1989).